Difference Scheme for the Vlasov-Manev System

R. Illner and S. Rjasanow

Received: January 22, 1999

Communicated by Alfred K. Louis

Abstract. We develop and test a finite difference scheme for the Vlasov-Manev Equation in one space and one velocity dimension. The Manev correction to the Newtonian potential produces visible qualitative differences in the behaviour of stellar systems; the most notable effect observed in this paper is a stabilisation of the separate identities of two Maxwellian concentrations at different locations.

1991 Mathematics Subject Classification: 65N06,65N12,65N22,85A05
Keywords and Phrases: Vlasov-Manev system, Finite difference methods, stability

1 Introduction

We are concerned with the numerical solution of the Vlasov equation with a Manev-type correction to the potential in $1+1$ (one space, one velocity) dimensions. In the three-dimensional case, the Newtonian potential is changed to the "Manev" potential

$$U(|x-y|) = -\frac{\gamma}{|x-y|} - \frac{\delta}{|x-y|^2}. \tag{1}$$

The correction $-\delta/|x-y|^2$ was introduced by Manev in a series of papers [7],[8],[9], [10] in the 1920s in an attempt to find a semiclassical approximation to the relativistic central force problem. For γ the universal gravitational constant and $\delta = 3\gamma^2/c^2$, where c is the speed of light, this correction gives a qualitatively accurate prediction of the precession of the perihelion of Mercury. Manev's work was the main motivation for the recent paper [2], in which the authors discuss the properties of the corresponding stellar dynamic equation. Notably, it is shown that the Cauchy problem for this equation does not, in general, admit global solutions (the corresponding result for the classical stellar dynamic equation holds only if the number of space dimensions is larger than or equal to 4, see, e.g., [4]). This means that a stellar system driven by Manev forces will typically develop features where the spatial density ρ loses smoothness such that the Manev force term, i.e., the Riesz transform of ρ

$$E_2[\rho](t,x) := -\delta \int \frac{x-y}{|x-y|^4}\rho(t,y)\,dy$$

diverges. Possible reasons for this are the local formation of singularities in ρ ("concentrations") or in $\nabla_x \rho$ (e.g., "shock waves"). As it is well known that such singularities do not occur in solutions of the classical stellar dynamic equation (see [4]), the Manev correction may be of physical relevance in modelling the evolution of large stellar systems like galaxies, globular clusters or interstellar dust clouds.

We remark that an equation with $\gamma = 0$ and $\delta > 0$ (referred to as the "pure" Manev case in [2]) possesses an interesting "projective" invariance in addition to the standard translation, scaling and Galilei invariances. Specifically, as shown in [2], if $f(t,x,v)$ is a solution of the pure Manev equation

$$\partial_t f + v \cdot \nabla_x f + E_2[\rho] \cdot \nabla_v f = 0$$

and if for some $a > 0$, $\tau = t/(1+at)$, $y = x/(1+at)$ and $w = (1+at)v - ax$, then

$$F(\tau, y, w) := f(t,x,v)$$

solves

$$\partial_\tau F + w \cdot \nabla_y F + E_2[\tilde{\rho}] \cdot \nabla_w F = 0$$

with $\tilde{\rho} = \int F\,dw$. This "projective" invariance, described in the context of the corresponding N-body problem by Bobylev and Ibragimov [1], may be of significance (and use) in regions where ρ or $\nabla\rho$ are large and the Manev correction dominates the Newtonian forces.

As also discussed in [2], Boltzmann collision terms are dimensionally of the same order as the Manev force term and should therefore be included in a proper model. However, the present study aims at the identification of effects which can be attributed to the Manev correction alone; we therefore omit Boltzmann collision terms and any other conceivable correction (such as, e.g., Smoluchowski type coagulation terms).

It is tempting to try a particle or particle-in-cell scheme for this equation, as is common for the Vlasov-Poisson (VP) system. The most advanced scheme of this type for VP is due to Greengard and Rokhlin [5]. We experimented with particle schemes for the Vlasov-Manev equation and found that they performed poorly due to the strong singularity of the Manev correction at very short range. Specifically, particles could be accelerated to extreme velocities over one time step, an effect which can also happen for VP but which is rare enough to cause no difficulties. It should also be an insignificant effect for the Vlasov-Manev equation while the densities are smooth (this follows from the existence and uniqueness proof shown in [6]), so a good numerical method should reflect this; but particle methods do not. Of course, one could mollify the Manev potential in order to avoid the difficulty, but unless the mollification parameter is chosen with great care, this may obfuscate the effects of the Manev correction relative to the Newtonian forces. It is for these reasons that we decided to avoid particle methods altogether.

The main objective of this paper is therefore the construction and testing of a difference scheme for the Vlasov-Manev (VM) equation in one-dimensional geometry; effective generalisation for multidimensional cases is planned for future work.

Our paper is organised as follows. In Section 2, we describe the VM equation and summarise its properties. In Section 3, a difference scheme for VM is derived, and its properties are formulated and proved. Section 4 contains a few informative numerical examples.

2 The Vlasov-Manev equation and its properties

The one-dimensional Vlasov-Manev equation is associated with the potential

$$U(|x-y|) = -\gamma|x-y| - \delta \ln|x-y|.$$

This potential arises from (1) by assuming homogeneity of the stellar system in the $y-$ and $z-$ directions, and the Vlasov-Manev equation can be written in the form

$$f_t + v\, f_x + E\, f_v = 0, \tag{2}$$

where $f = f(t,x,v) : \mathbb{R}_+ \times \mathbb{R}_x \times \mathbb{R}_v \to \mathbb{R}_+$ is a non-negative distribution density function, $t \geq 0$ is the time variable, x is the space variable and v is the velocity variable. The force function $E = E(t,x)$ is defined as follows:

$$\begin{aligned} E(t,x) &= -\gamma \int_{\mathbb{R}_y} \frac{x-y}{|x-y|}\rho(t,y)dy - \delta \int_{\mathbb{R}_y} \frac{x-y}{|x-y|^2}\rho(t,y)dy, \qquad (3) \\ \rho(t,x) &= \int_{\mathbb{R}_v} f(t,x,v)dv. \end{aligned}$$

or $E = -\nabla U$, with

$$U(t,x) = -\gamma \int |x-y|\rho(t,y)\, dy - \delta \int \ln|x-y|\rho(t,y)\, dy.$$

Here, ρ denotes the spatial density. The non-negative constants γ and δ are given, and typically $\gamma >> \delta$. The equation (2) is complemented with the initial condition

$$f(0,x,v) = f_0(x,v) \geq 0. \tag{4}$$

We summarise the main properties of this equation.

1. Conservation of non-negativity

$$\text{if } f_0(x,v) \geq 0, \text{ then for } t > 0 \quad f(t,x,v) \geq 0.$$

2. Conservation of mass

$$m(t) = \int_{\mathbb{R}_x} \int_{\mathbb{R}_v} f(t,x,v) dv dx = m(0) = \int_{\mathbb{R}_x} \int_{\mathbb{R}_v} f_0(x,v) dv dx.$$

3. The continuity equation reads

$$\begin{aligned} \rho_t(t,x) &+ j_x(t,x) = 0, \\ j(t,x) &= \int_{\mathbb{R}_v} v\, f(t,x,v) dv. \end{aligned} \tag{5}$$

4. Conservation of energy

$$\begin{aligned} e(t) &= \frac{1}{2} \int_{\mathbb{R}_v} \int_{\mathbb{R}_x} v^2 f(t,x,v) dx dv \\ &- \frac{1}{2} \int_{\mathbb{R}_x} \int_{\mathbb{R}_y} (\gamma |x-y| + \delta \ln |x-y|) \rho(t,x) \rho(t,y) dx dy = e(0). \end{aligned}$$

5. Second derivative of the moment of inertia

$$\begin{aligned} \frac{d^2}{dt^2} \int_{\mathbb{R}_x} x^2 \rho(t,x) dx &= 2 \int_{\mathbb{R}_x} \int_{\mathbb{R}_v} v^2 f(t,x,v)\, dv\, dx \\ &- \gamma \int_{\mathbb{R}_x} \int_{\mathbb{R}_y} |x-y| \rho(t,x) \rho(t,y) dy\, dx - \delta\, m^2(0). \end{aligned}$$

In the three-dimensional case and for $\gamma = 0$, the last identity is

$$\frac{d^2}{dt^2} \int x^2 \rho(t,x)\, dx = 4e(0),$$

and this can be used to show non-global existence (for $\gamma = 0$) whenever the initial energy is negative. This argument is not applicable in the one-dimensional case under consideration; it may well be that solutions in this situation always exist globally.

3 A difference scheme

We begin our numerical study of the initial value problem (2),(4) with the discretisation of the physical and velocity spaces. First, we restrict the whole space $\mathbb{R}_x \times \mathbb{R}_v$ to a rectangle

$$Q_L = \{(x,v) \in \mathbb{R}_x \times \mathbb{R}_v,\ -L_x \le x \le L_x,\ -L_v \le v \le L_v\},$$

and assume that $f(t,x,v)$ has its support with respect to x and v in the box Q_L. We can then compute the force field by integrating over Q_L alone; later, we shall act as if f is extended periodically in x and v.
The next step is the discretisation of the rectangle Q_L using the nodes

$$\begin{aligned}
(x_i, v_j) &= (-L_x + i\, h_x, -L_v + j\, h_v),\ (i,j) \in Q_n \\
h_x &= \frac{2L_x}{n_x},\ n_x \in \mathbb{N},\ \text{and } n_x \text{ is even}, \\
h_v &= \frac{2L_v}{n_v},\ n_v \in \mathbb{N},\ \text{and } n_v \text{ is even}, \\
Q_n &= \{(i,j) \in \mathbb{Z}^2,\ 0 \le i \le n_x,\ 0 \le j \le n_v\}.
\end{aligned}$$

Furthermore, we introduce the index set $\tilde{Q}_n$ as a subset of all vectors in Q_n excluding those which have the form $(0,j)$ or $(i,0)$.
Let $\tau > 0$ be the time discretisation parameter, and $t_k = k\,\tau,\ k = 0,1,\ldots.$ The function $f(t_k,x,v)$ will now be represented by a vector $f^k \in \mathbb{R}^n,\ n = n_x\, n_v$ with components

$$f_l^k = f_{i,j}^k \approx f(t_k, x_i, v_j),\ (i,j) \in \tilde{Q}_n. \tag{6}$$

Here, l denotes the global index of the vector f^0, given by

$$l = (j-1)\, n_x + i,\ l = 1,\ldots,n.$$

Note that (6) defines the vector f^k for all $(i,j) \in Q_n$ by the assumed periodic extension of f.
It is also convenient to use the matrix form of the unknown function:

$$F^k \in \mathbb{R}^{n_x \times n_v}.$$

The numerical density $\rho_i^k \approx \rho(t_k, x_i)$ can be computed using the midpoint integration rule

$$\begin{aligned}\rho_i^k &= h_v \sum_{j=1}^{n_v} f_{i,j}^k,\ i = 1, \ldots, n_x, \\ \rho_0^k &= \rho_{n_x}^k,\ k = 0, 1, \ldots,\end{aligned}$$

or in the matrix form

$$\rho^k = h_v F^k e_{n_v}, \tag{7}$$

where $\rho^k \in \mathbb{R}^{n_x}$ and $e_{n_v} = (1, \ldots, 1)^T \in \mathbb{R}^{n_v}$.
The total mass of the system is

$$m^k = h_x \sum_{i=1}^{n_x} \rho_i^k$$

and can be computed as follows:

$$m^k = h_x \left(\rho^k, e_{n_x}\right) = h_x\, h_v\, \left(f^k, e_n\right) = h_x\, h_v\, \left(F^k e_{n_v}, e_{n_x}\right). \tag{8}$$

The next and most involved step is the numerical computation of the force due to (3). We take advantage of the fact that it is sufficient to integrate over one spatial period in (3), because what is really done is treat the case where the support of ρ stays inside such a period.
Using the notation

$$P(x-y) = -\gamma \frac{x-y}{|x-y|} - \delta \frac{x-y}{|x-y|^2}$$

and the piecewise representation of the density ρ we compute

$$E(t_k, x_i) \approx E_i^k = \sum_{j=1}^{n_x} \rho_j^k G_{ij}, \tag{9}$$

$$E^k = G\, \rho^k,\ E^k \in \mathbb{R}^{n_x},\ G \in \mathbb{R}^{n_x \times n_x}. \tag{10}$$

The elements of the matrix G are defined by

$$G_{ij} = \int_{x_j - h_x/2}^{x_j + h_x/2} P(x_i - y) dy. \tag{11}$$

Direct computation of the force via (9) will require $O(n_x^2)$ arithmetical operations in each time step and is therefore an "expensive" step. The combination of the special form of the matrix G and uniform discretisation leads to a special, Toeplitz form of the matrix G.

Lemma 1 *The matrix G defined in (11) is a skew-symmetric Toeplitz matrix.*

Proof:
A matrix G is Toeplitz if

$$G_{i+1,j+1} \quad = \quad G_{ij},\ i,j = 1,\ldots,n_x - 1.$$

The analytical integration in (11) leads to

$$G_{ij} = \gamma\, h_x - \delta\, \ln \frac{j - i - 1/2}{j - i + 1/2},\ j > i.$$

For $j < i$ we get

$$G_{ij} = -G_{ji}$$

because of (11).
The matrix G is therefore uniquely defined by its first row. The element G_{11} is a strongly singular integral which should be considered as a Cauchy integral

$$G_{11} = \lim_{\varepsilon \to 0} \left(\int_{x_1 - h_x/2}^{x_1 - \varepsilon} P(x_1 - y) dy + \int_{x_1 + \varepsilon}^{x_1 + h_x/2} P(x_1 - y) dy \right).$$

Using the substitution $y = -y' + 2x_1$ in the second integral and the obvious property

$$P(x - y) = -P(y - x)$$

we obtain

$$\begin{aligned}\int_{x_1+\varepsilon}^{x_1+h_x/2} P(x_1-y)dy &= -\int_{x_1-\varepsilon}^{x_1-h_x/2} P(x_1+y'-2x_1)dy' \\ &= \int_{x_1-h_x/2}^{x_1-\varepsilon} P(y'-x_1)dy' \\ &= -\int_{x_1-h_x/2}^{x_1-\varepsilon} P(x_1-y')dy',\end{aligned}$$

and therefore

$$G_{11} = 0.$$

■

Remark 1 *The multiplication of a Toeplitz matrix with a vector can be realised efficiently using the following well known trick. The matrix G can be considered as a left-upper block of the circulant matrix $\tilde{G}$ of the dimension m which is a power of two:*

$$\tilde{G} = \begin{pmatrix} G & G_{12} \\ G_{21} & G_{22} \end{pmatrix},$$

The matrix $\tilde{G}$ has the following additional property

$$\tilde{G}_{i,m} \quad = \quad \tilde{G}_{i+1,1}, \;\; i = 1, \ldots, m-1$$

and its first row is defined as

$$(G_{11}, \ldots, G_{1,n_x}, 0, \ldots, 0, -G_{n_x,1}, -G_{n_x-1,1}, \ldots, -G_{2,1}) \in \mathbb{R}^{1\times m}. \tag{12}$$

The dimension m of the matrix $\tilde{G}$ is the next power of two for the number $2\,n_x-1$ and the number of zeros in (12) is equal to $m-2n_x+1$. It is obviously true that $2\,n_x-1 < m < 4\,n_x-4$.
Each circulant matrix C of the dimension m can be represented as

$$C = m^{-1} F_m \,\Lambda\, F_m^*,$$

where F_m denotes the matrix of the Discrete Fourier Transform (DFT) of the dimension m. The diagonal matrix Λ contains the eigenvalues of C and can be computed as

$$\Lambda = diag(\lambda_1, \ldots, \lambda_m) = diag(F_m C^T e_1), \tag{13}$$

e.g. as the DFT of the first row of the matrix C.

The computation of the force due to (10) therefore reduces to one DFT in a preparatory step for the computation of the eigenvalues of the matrix $\tilde{G}$ using (13) (the matrix $\tilde{G}$ remains fixed during the time steps), and then to two DFTs and one multiplication of the diagonal matrix $n_x^{-1}\Lambda$ with a vector. If m is a power of two then the computation of the force only requires $O(n_x \log_2(n_x))$ arithmetical operations using the Fast Fourier Transform (FFT) [3],[13] and is therefore much "cheaper" than the computation of the density via (7) which requires $O(n) = O(n_x\, n_v)$ arithmetical operations. The number of arithmetical operations for the multiplication

$$\tilde{G}\tilde{\rho}^k = \begin{pmatrix} G & G_{12} \\ G_{21} & G_{22} \end{pmatrix} \begin{pmatrix} \rho_k \\ 0 \end{pmatrix} = \begin{pmatrix} G\,\rho_k \\ G_{21}\,\rho_k \end{pmatrix} \tag{14}$$

is then of the same order $O(n_x \log_2(n_x))$.

Remark 2 *In a two- $(d=2)$ or three-dimensional case $(d=3)$ we will obtain a circulant-block matrix [12]. Such matrices can again be efficiently multiplied with a vector using the FFT. The amount of arithmetical work would be $O(n_x^d \log_2(n_x))$ in this case.*

The next step in the numerical procedure we are describing is the discretisation of the equation (2) using a semi-implicit difference scheme. At the given time level k we compute the density ρ^k via (7) and the force E^k via (10) or (14), and then we use the following "upwind" approximation for the derivatives in (2):

$$f_t(t_k, x_i, v_j) \approx f^k_{t,ij} = \frac{f^{k+1}_{ij} - f^k_{ij}}{\tau}, \tag{15}$$

$$v\, f_x(t_k, x_i, v_j) \approx v_j\, f^{k+1}_{x,ij} = \begin{cases} v_j \dfrac{f^{k+1}_{ij} - f^{k+1}_{i-1,j}}{h_x} &, \quad v_j \geq 0 \\ v_j \dfrac{f^{k+1}_{i+1,j} - f^{k+1}_{ij}}{h_x} &, \quad v_j < 0 \end{cases}, \tag{16}$$

$$E\, f_v(t_k, x_i, v_j) \approx E^k_i\, f^{k+1}_{v,ij} = \begin{cases} E^k_i \dfrac{f^{k+1}_{ij} - f^{k+1}_{i,j-1}}{h_v} &, \quad E^k_i \geq 0 \\ E^k_i \dfrac{f^{k+1}_{i,j+1} - f^{k+1}_{ij}}{h_v} &, \quad E^k_i < 0 \end{cases}. \tag{17}$$

The resulting difference scheme can now be written in the form

$$f^k_{t,ij} + v_j\, f^{k+1}_{x,ij} + E^k_i\, f^{k+1}_{v,ij} = 0,\ i,j \in \tilde{Q}_n,\ k = 0,1,\dots\ . \tag{18}$$

The initial values $f^0_{ij} = f_0(x_i, v_j)$ are given. After multiplication by τ, (18) is a system of linear equations which can be written in the matrix form

$$A_k\, f^{k+1} = f^k,\ A_k \in \mathbb{R}^{n\times n},\ f^k, f^{k+1} \in \mathbb{R}^n,\ n = n_x\, n_v.$$

The elements of the matrix A_k using the global numbering with $l = n_x(j-1)+i$ are of the form

$$
\begin{aligned}
(A_k)_{ll} &= 1 + \frac{\tau}{h_x}|v_j| + \frac{\tau}{h_v}|E_i^k|, && (19)\\
(A_k)_{l,l-1} &= \begin{cases} -\frac{\tau}{h_x}|v_j| & , \quad v_j \geq 0 \\ 0 & , \quad v_j < 0 \end{cases}, && (20)\\
(A_k)_{l,l+1} &= \begin{cases} 0 & , \quad v_j \geq 0 \\ -\frac{\tau}{h_x}|v_j| & , \quad v_j < 0 \end{cases}, && (21)\\
(A_k)_{l,l-n_x} &= \begin{cases} -\frac{\tau}{h_v}|E_i^k| & , \quad E_i^k \geq 0 \\ 0 & , \quad E_i^k < 0 \end{cases}, && (22)\\
(A_k)_{l,l+n_x} &= \begin{cases} 0 & , \quad E_i^k \geq 0 \\ -\frac{\tau}{h_v}|E_i^k| & , \quad E_i^k < 0 \end{cases}, && (23)\\
l &= 1, \ldots, n\ .
\end{aligned}
$$

All other elements of the matrix A_k are equal to zero, i.e. the matrix A_k is extremely sparse. Exactly three elements of each row of this matrix are unequal to zero. In a $d-$dimensional case this number would be $2d+1$.

Remark 3 *If the indices in (15)-(17) or in (20)-(24) are not from the set* $\tilde{Q}_n$ *then we always assume the periodic property (e.g.* $f^{k+1}_{n_x+1,j} \equiv f^{k+1}_{1,j}$ *etc.).*

The main properties of the difference scheme (18) correspond to the properties of the matrices $A_k,\ k = 0, \ldots\ .$

Lemma 2 *The matrix* A_k *has the following properties*

1. A_k *is a regular M-matrix,*
2. $A_k\, e_n = e_n,\ A_k^T\, e_n = e_n,$
3. $\|A_k^{-1}\|_2 = 1.$

Here $\|A_k^{-1}\|_2$ *denotes the spectral norm of the matrix* A_k^{-1}*, i.e. its biggest singular value.*

Proof:

1. The elements of the matrix A_k fulfil

$$\begin{aligned} (A_k)_{ll} &> 0,\ (A_k)_{lm} \leq 0,\ l \neq m, \\ \sum_{m=1}^{n} (A_k)_{lm} &= 1,\ l = 1, \ldots, n. \end{aligned} \tag{24}$$

   By (24), the matrix A_k is strongly diagonal-dominant and therefore a regular $M-$matrix.

2. The first property is given trivially in (24). This means that the vector e_n is an eigenvector of the matrix A_k and corresponds to the eigenvalue one. The matrix A_k^T has the same eigenvector and the same eigenvalue because

$$\begin{aligned} \left(A_k^T\, e_n\right)_l &= \sum_{m=1}^{n} (A_k)_{ml} = \\ &= (A_k)_{ll} + (A_k)_{l+1,l} + (A_k)_{l-1,l} + (A_k)_{l-n_x,l} + (A_k)_{l+n_x,l}\,. \end{aligned}$$

   Using the representations $(l+1,l) = (l+1,(l+1)-1)$ and $(l-1,l) = (l-1,(l-1)+1)$, the property $l \pm 1 = (n_x - 1)j + (i \pm 1)$ and (20),(21) we obtain

$$(A_k)_{l+1,l} + (A_k)_{l-1,l} = -\frac{\tau}{h_x}|v_j|.$$

   By analogy

$$(A_k)_{l-n_x,l} + (A_k)_{l+n_x,l} = -\frac{\tau}{h_v}|E_i^k|.$$

   Together with (19) we obtain the required result.

3. The matrix A_k^{-1} is element-wise non-negative, because it is the inverse of the $M-$matrix. The spectral norm of the matrix A_k^{-1} is equal to its largest singular value or to the square root of the largest eigenvalue of the matrix $A_k^{-T} A_k^{-1}$. This matrix only has non-negative elements (as a product of two element-wise non-negative matrices) and the real eigenvector e_n only has positive components. Then the corresponding eigenvalue (Perron-Frobenius theorem) is the largest Perron-eigenvalue of this matrix. In our case this eigenvalue is equal to one, because of the properties in 2. Hence the spectral norm of the matrix A_k^{-1} is equal to one.

■

More details concerning $M-$matrices can be found in [11].
The above lemma enables us to prove some important properties of the difference scheme

$$
\begin{array}{ll}
1. & \text{Initial step} \\
 & f_{ij}^0 = f_0(x_i, v_j), \\
2. & \text{Time step for } k = 0, 1, \dots \\
2.1 & \rho^k = h_v\, F^k\, e_{n_v}, \\
2.2 & E^k = G\,\rho^k, \\
2.3 & A_k f^{k+1} = f^k.
\end{array}
\tag{25}
$$

Corollary 1 *The solution of the difference scheme (25) exists for all* $k = 0, 1\dots$.

Proof: This property follows directly from the regularity of the matrix A_k for all $k = 0, 1\dots$.

■

Corollary 2 *If the initial function* $f_0(x, v)$ *is non-negative then the vectors* f^k *remain component-wise non-negative for all* $k = 0, 1, \dots$.

Proof:
The initial vector f^0 is component-wise non-negative because of its definition in step 1 of (25). If $f^k,\ k = 0, 1, \dots$ is component-wise non-negative, then we obtain from Step 2.3 of (25)

$$f^{k+1} = A_k^{-1} f^k.$$

The matrix A_k^{-1} is component-wise non-negative because it is inverse of an M-matrix. The proof is then completed by induction.

■

Corollary 3 *The difference scheme (25) conserves mass.*

Proof:
The mass of the system can be computed for $k = 1, 2, \dots$ corresponding to formula (8)

$$
\begin{aligned}
m^k &= h_x h_v (f^k, e_n) = h_x h_v (A_{k-1} f^{k-1}, e_n) \\
&= h_x h_v (f^{k-1}, A_{k-1}^T e_n) = h_x h_v (f^{k-1}, e_n) = m^{k-1} = \dots = m^0.
\end{aligned}
$$

■

Corollary 4 *The difference scheme (25) is stable in the discrete maximum norm with respect to the initial data.*

Proof: The discrete maximum norm of $f^k,\ k = 0, 1, \dots$ is defined as

$$\|f^k\|_\infty = \max_l |f_l^k| = \max_l f_l^k = f_{l^*}^k$$

because the components of the vector f^k are non-negative. Here we have used the global numbering $l = n_x(j-1) + i$ of the components of f^k. Using

$$(A_{k-1})_{l^* l^*} > 0,\ (A_{k-1})_{ij} \le 0,\ i \ne j$$

in the time step $k = 1, 2, \dots$ we obtain the following estimate for the index l^*

$$\begin{aligned}
\|f^k\|_\infty &= f_{l^*}^k = ((A_{k-1})_{l^*l^*} + (A_{k-1})_{l^*l^*-1} \\
&+ (A_{k-1})_{l^*l^*+1} + (A_{k-1})_{l^*l^*-n_x} + (A_{k-1})_{l^*l^*+n_x})\, f_{l^*}^k \\
&\le (A_{k-1})_{l^*l^*} f_{l^*}^k + (A_{k-1})_{l^*l^*-1} f_{l^*-1}^k \\
&+ (A_{k-1})_{l^*l^*+1} f_{l^*+1}^k + (A_{k-1})_{l^*l^*-n_x} f_{l^*-n_x}^k + (A_{k-1})_{l^*l^*+n_x} f_{l^*+n_x}^k = \\
&+ (A_{k-1} f^k)_{l^*} = f_{l^*}^{k-1} \le \|f^{k-1}\|_\infty \le \dots \le \|f^0\|_\infty.
\end{aligned}$$

■

Corollary 5 *The difference scheme (25) is stable in the discrete L_2-norm with respect to the initial data.*

Proof: The discrete L_2-norm of $f^k,\ k = 0, 1, \dots$ is defined as

$$\|f^k\|_2^2 = h_x h_v (f^k, f^k).$$

Using this definition and property 3 in Lemma 2 we obtain for $k = 1, \dots$

$$\|f^k\|_2 = \|A_{k-1}^{-1} f^{k-1}\|_2 \le \|A_{k-1}^{-1}\|_2 \|f^{k-1}\|_2 = \|f^{k-1}\|_2 \le \dots \le \|f^0\|_2.$$

■

Corollary 6 *If the sequence $\{f^k\}$ converges then it converges to the constant*

$$\lim_{k\to\infty} f^k = \frac{m^0}{4L_xL_v}\, e_n$$

Proof: If the sequence $\{f^k\}$ converges to f^∞ then this vector fulfils

$$A_\infty f^\infty = f^\infty,$$

where A_∞ denotes the limit of the sequence of matrices $\{A_k\}$. Since the matrix A_∞ is still a regular $M-$matrix, its eigenvalue 1 is simple. It means that only a constant vector $f^\infty = \alpha e_n$ can fulfil the equation (26). The constant α can be obtained using the conservation of mass

$$m^0 = h_x h_v (f^\infty, e_n) = h_x h_v \alpha (e_n, e_n) = \alpha (h_x n_x)(h_v n_v) = \alpha (4 L_x L_v).$$

■

Next, we obtain the discrete form of the continuity equation (5). We will use the following notations

$$\begin{array}{lll}
v = (v_1, \ldots, v_{n_v})^T \in \mathbb{R}^{n_v} & \text{– vector of the velocities,} & \\
D_v = \mathrm{diag}(v) \in \mathbb{R}^{n_v \times n_v} & \text{– corresponding diagonal matrix,} & \\
D_v^+ = \mathrm{diag}(0.5(|v| + v)) \in \mathbb{R}^{n_v \times n_v} & \text{– positive part of } D_v, & \\
D_v^- = \mathrm{diag}(0.5(|v| - v)) \in \mathbb{R}^{n_v \times n_v} & \text{– negative part of } D_v, & \\
w = (v_1^2, \ldots, v_{n_v}^2)^T \in \mathbb{R}^{n_v} & \text{– vector of squares of the velocities,} & \\
E^k = (E_1^k, \ldots, E_{n_x}^k)^T \in \mathbb{R}^{n_x} & \text{– vector of the forces,} & (*) \\
D_E = \mathrm{diag}(E^k) \in \mathbb{R}^{n_x \times n_x} & \text{– corresponding diagonal matrix,} & \\
D_E^+ = \mathrm{diag}(0.5(|E^k| + E^k)) \in \mathbb{R}^{n_x \times n_x} & \text{– positive part of } D_x, & \\
D_E^- = \mathrm{diag}(0.5(|E^k| - E^k)) \in \mathbb{R}^{n_x \times n_x} & \text{– negative part of } D_v, & \\
J_m = \mathrm{circ}(0, 1, 0, \ldots, 0) \in \mathbb{R}^{m \times m} & \text{– circulant matrix of the dimension } m, & \\
\rho^k = h_v \, F^k \, e_{n_v} \in \mathbb{R}^{n_x} & \text{– density,} & \\
j^k = h_v \, F^k \, v \in \mathbb{R}^{n_x} & \text{– numerical flux.} &
\end{array}$$

Using $(*)$ we rewrite the difference scheme (18) in the matrix form

$$\begin{aligned}
\frac{F^{k+1} - F^k}{\tau} \quad &+ \quad \frac{1}{h_x} \left((I_{n_x} - J_{n_x}) F^{k+1} D_v^- + (I_{n_x} - J_{n_x}^T) F^{k+1} D_v^+ \right) \\
&+ \quad \frac{1}{h_v} \left(D_E^- F^{k+1} (I_{n_v} - J_{n_v}^T) + D_E^+ F^{k+1} (I_{n_v} - J_{n_v}) \right) = 0, \\
k \quad &= \quad 0, 1, \ldots \, .
\end{aligned}$$

If we multiply this matrix with the vector $h_v e_{n_v}$ then we obtain using

$$\begin{aligned}
(I_{n_v} - J_{n_v}) e_{n_v} &= (I_{n_v} - J_{n_v}^T) e_{n_v} = 0, \\
D_v^- e_{n_v} &= v^-, \\
D_v^+ e_{n_v} &= v^+
\end{aligned}$$

the following equation

$$\frac{\rho^{k+1} - \rho^k}{\tau} + \frac{h_v}{h_x} \left((I_{n_x} - J_{n_x}) F^{k+1} v^- + (I_{n_x} - J_{n_x}^T) F^{k+1} v^+ \right),$$

$$\frac{\rho^{k+1}-\rho^k}{\tau} + \frac{h_v}{h_x}\big(0.5(I_{n_x}-J_{n_x})F^{k+1}(|v|-v)+0.5(I_{n_x}-J_{n_x}^T)F^{k+1}(|v|+v)\big),$$
$$\frac{\rho^{k+1}-\rho^k}{\tau} + \frac{1}{2h_x}(J_{n_x}-J_{n_x}^T)j^{k+1}+\frac{1}{2}h_xh_v\frac{1}{h_x^2}(2I_{n_x}-J_{n_x}-J_{n_x}^T)F^{k+1}|v| = 0$$

or

$$\frac{\rho^{k+1}-\rho^k}{\tau} + \frac{1}{2h_x}(J_{n_x}-J_{n_x}^T)j^{k+1} = -\frac{1}{2}h_xh_v\frac{1}{h_x^2}(2I_{n_x}-J_{n_x}-J_{n_x}^T)F^{k+1}|v|.$$

The short form of this equation is

$$\rho_t^k + j_{\dot{x}} = -\frac{1}{2}h_x(h_vF^{k+1}|v|)_{xx}, \tag{26}$$

where y_x denotes the central difference and y_{xx} the second difference of the grid function y. The equation (26) corresponds to the continuous equation (5). While the left hand side of (26) is a possible correct approximation of the derivatives in (5), the right hand side forms an artificial viscosity of our scheme. Because of this term which is of the order $O(h_x)$ we are not able to obtain the conservation of the energy of the scheme directly. However, our numerical tests show that the variation of the energy in one time step is small.

4 Numerical examples

In this section we calculate some examples using our difference scheme. The initial distribution $f_0(x,v)$ is given by

$$f_0(x,v) = \frac{1}{2\pi\sqrt{T_xT_v}}\left(\exp\left(-\frac{(x-x_0)^2}{2T_x}\right)+\exp\left(-\frac{(x+x_0)^2}{2T_x}\right)\right)\exp\left(-\frac{v^2}{2T_v}\right),$$

where T_x, T_v and x_0 are some positive parameters. In Figures 1,2 we present the time evolution of the density and of the force in the time interval $(0,1.4)$ for the following setting of parameters: $\gamma=4,\ \delta=0,\ T_x=2,\ T_v=0.05,\ x_0=4$ and $n_x=60,\ n_v=90$, i.e. for the pure Vlasov case. The time interval $(0,1.4)$ is sufficient to show the main numerical effects.

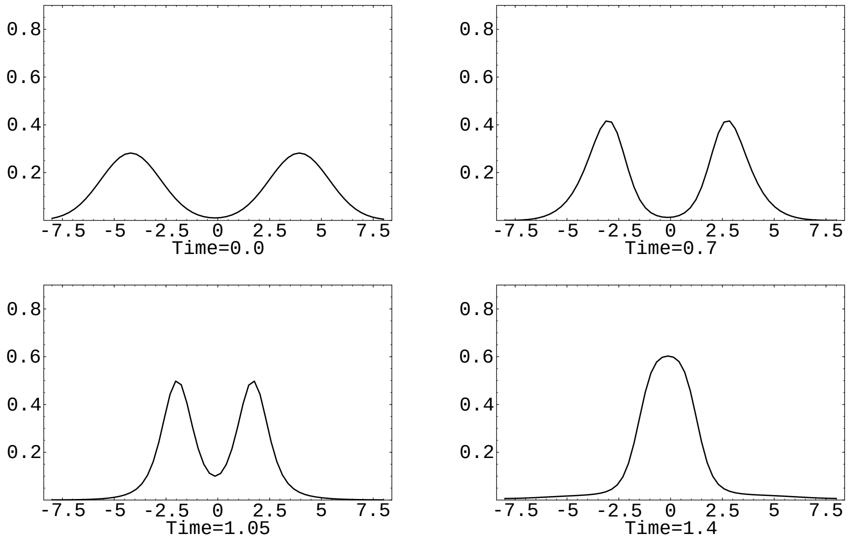

Figure 1: The density profiles for $\gamma = 4$, $\delta = 0$

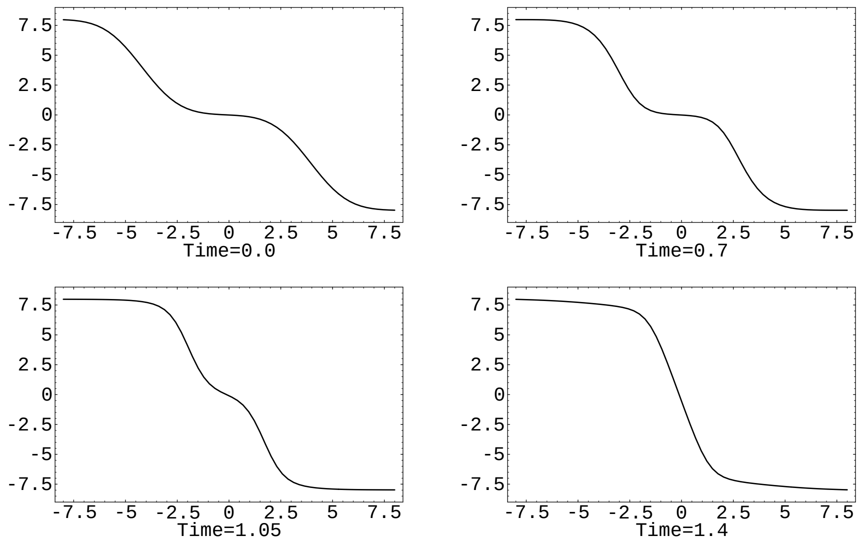

Figure 2: The force profiles for $\gamma = 4$, $\delta = 0$

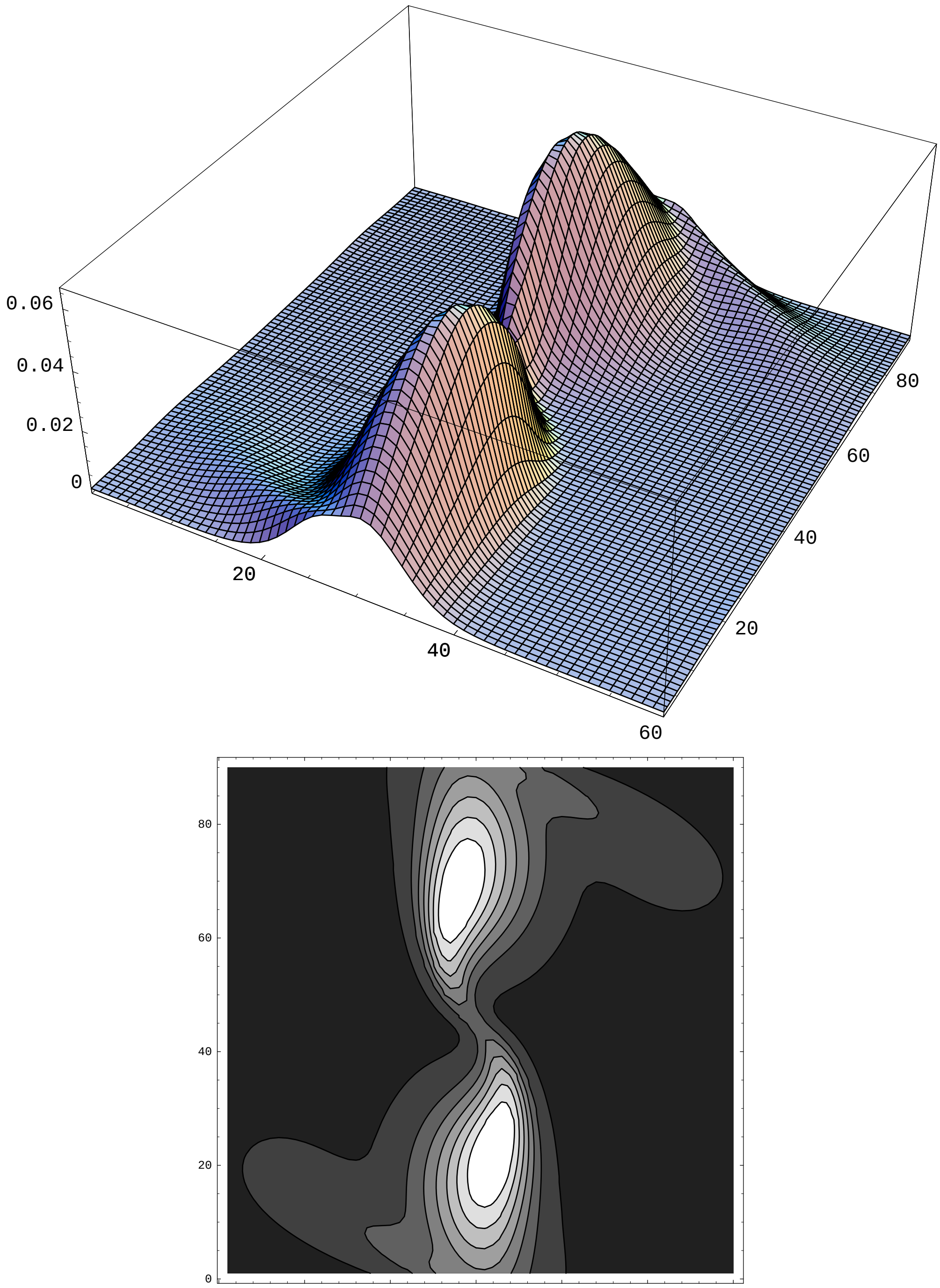

Figure 3: The solution and its iso-lines for $\gamma = 4$, $\delta = 0$

We observe a very clear unification of the two particle "clouds" in space and no remarkable concentration of mass during the time evolution. Figure 3 shows the function $f(t,x,v)$ and its iso-lines for the time $t = 1.4$.
In the second test we consider the pure Manev case with the same initial distribution and the same parameter of discretisation.

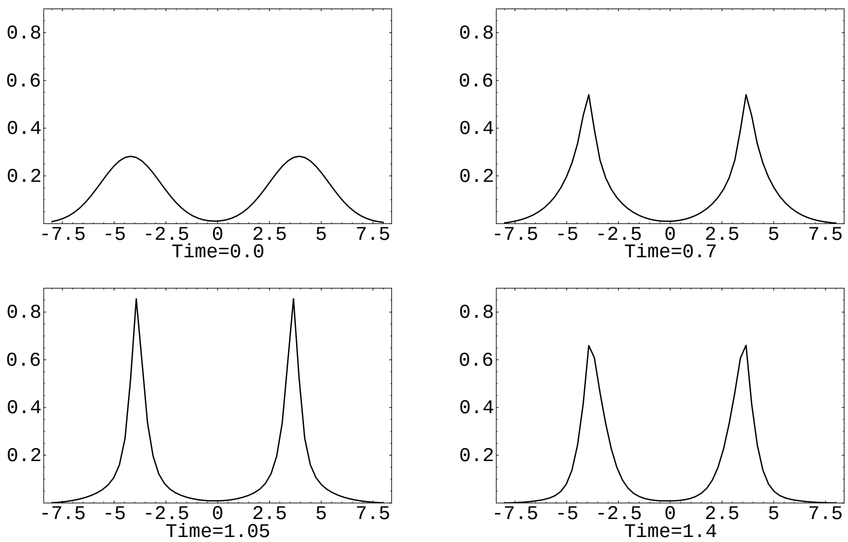

Figure 4: The density profiles for $\gamma = 0$, $\delta = 4$

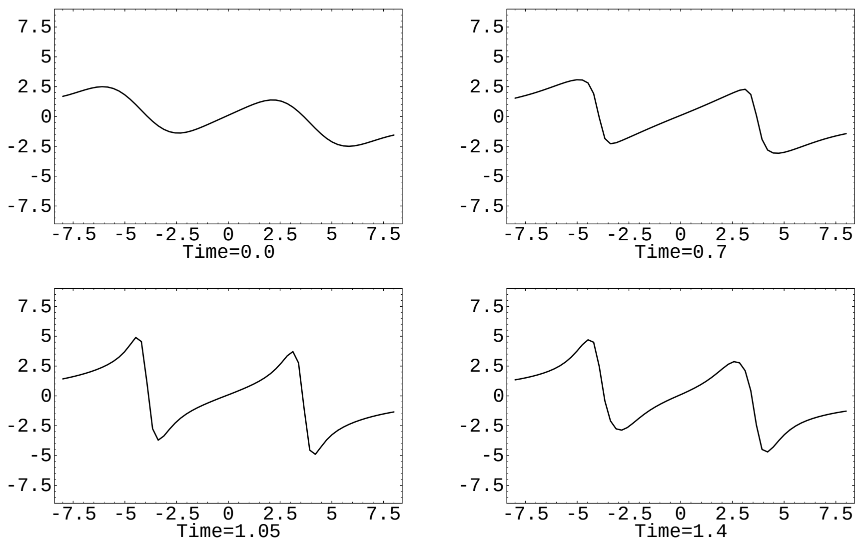

Figure 5: The force profiles for $\gamma = 0$, $\delta = 4$

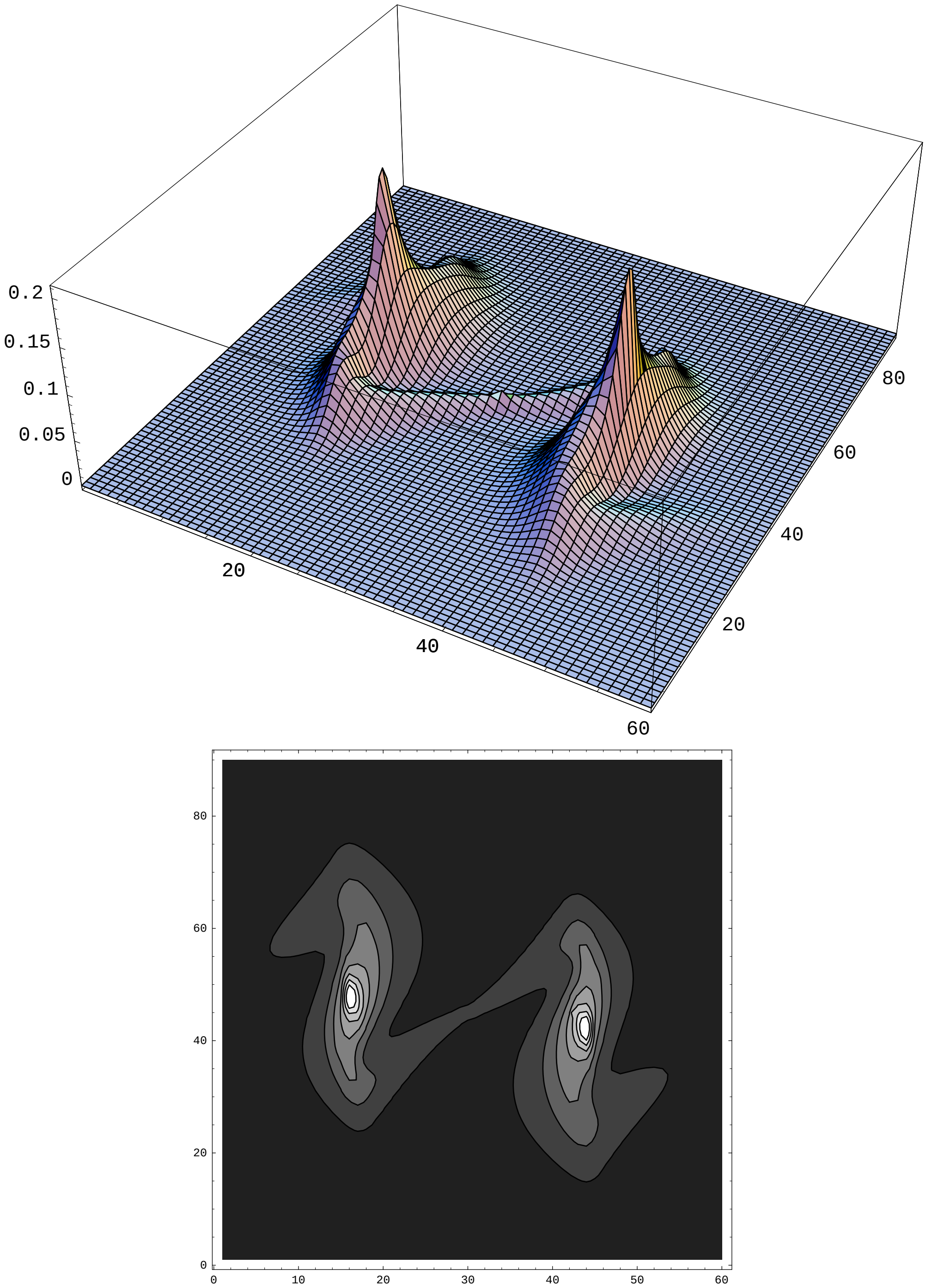

Figure 6: The solution and its iso-lines for $\gamma = 0$, $\delta = 4$

There is a very clear difference in the behaviour of the two examples. The pure Manev case leads to a significant concentration of the mass in the two “clouds”, and during the evolution they remain separated. Figure 6 shows the function $f(t,x,v)$ and its iso-lines for the time $t=1.4$.
Finally, we consider the mixed case $\gamma = 2,\ \delta = 2$ in order to illustrate the influence of the two effects: unification and concentration. The results are presented in Figures 7,8,9.

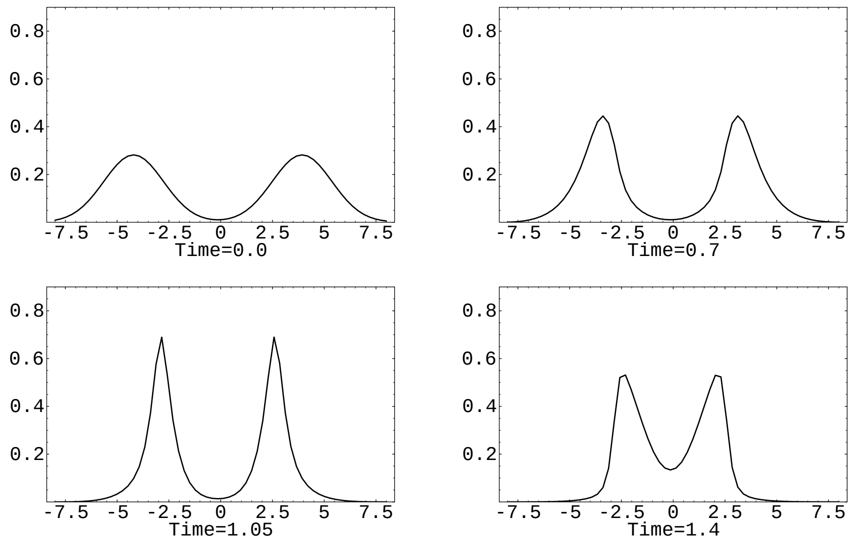

Figure 7: The density profiles for $\gamma = 2$, $\delta = 2$

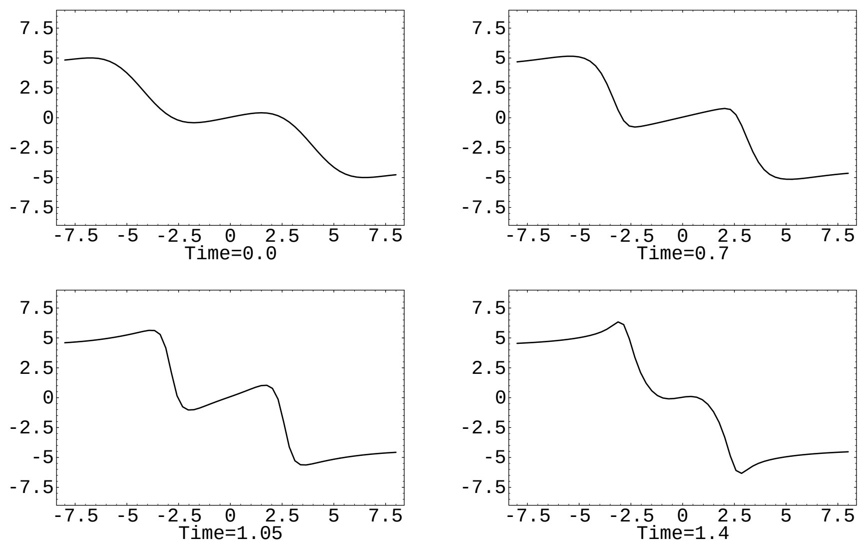

Figure 8: The force profiles for $\gamma = 2$, $\delta = 2$

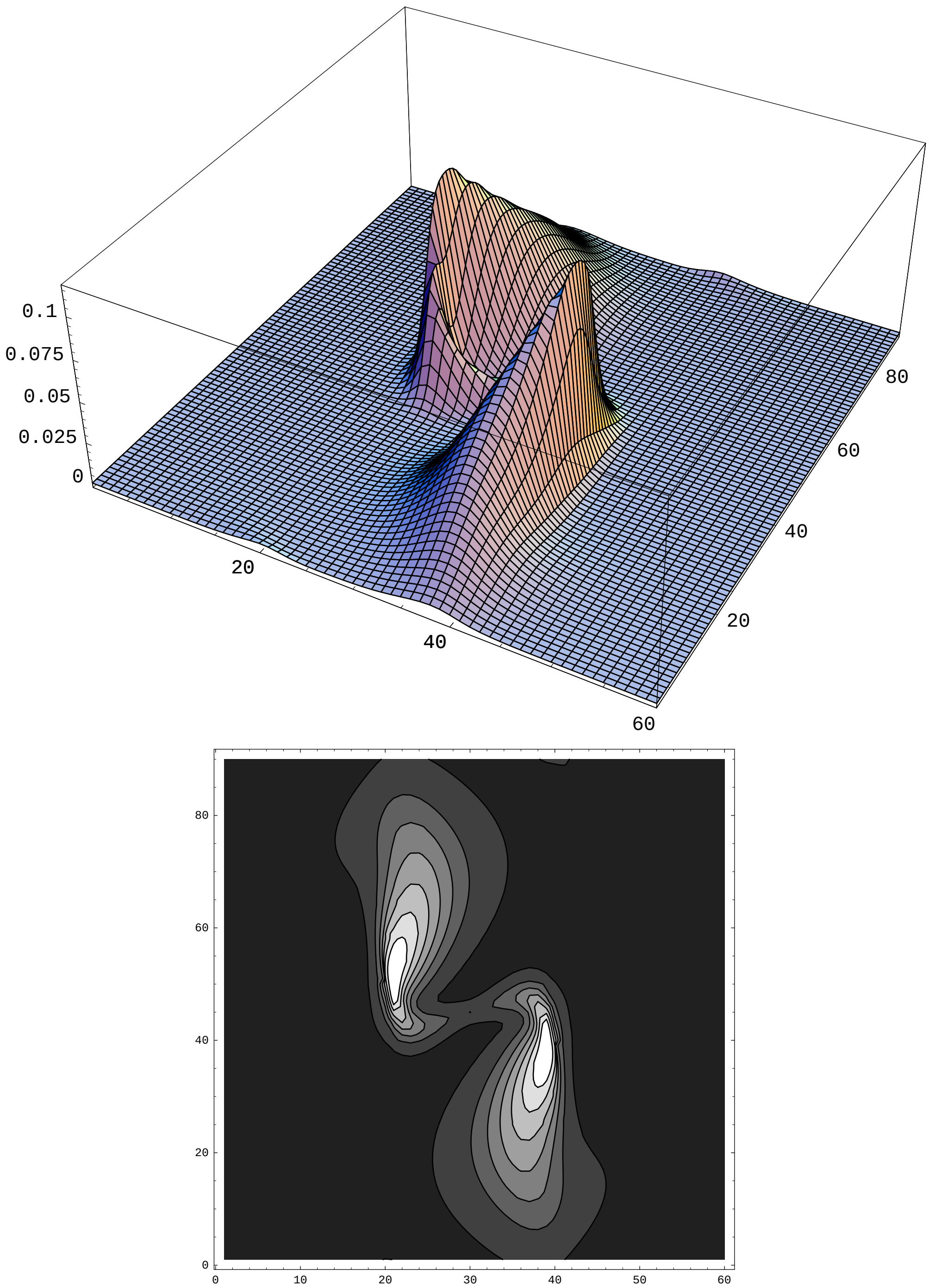

Figure 9: The solution and its iso-lines for $\gamma = 2$, $\delta = 2$

5 Conclusions

Our calculations suggest that the Manev correction will have a "stabilising" effect on isolated one-dimensional matter concentrations; this effect counteracts the tendency of the long-range Newtonian potential to accumulate all matter in one location; while this is only an isolated phenomenon which is observed here as a consequence of the Manev correction, we believe it to be evidence that truly interesting effects may occur in the more relevant three-dimensional case. Numerical experiments to this end are planned.

References

[1] A. Bobyblev and N. Ibragimov. The relationship of the group symmetry properties in dynamics, kinetic theory and hydrodynamics series. *Mathem. Modelirovanie*, 1 : 100–109, 1989.

[2] A. V. Bobylev, P. Dukes, R. Illner, and H. D. Victory. On Vlasov-Manev equations, I: Foundations, Properties and Global Nonexistence. *JSP*, 88:885–911, 1997.

[3] J. W. Cooley and J. W. Tukey. An algorithm for the machine calculation of complex Fourier series. *Math. Comput.*, 19 : 297–301, 1965.

[4] R. Glassey. *The Cauchy Problem in Kinetic Theory.* SIAM Publ., 1996.

[5] L. Greengard and V. Rokhlin. A Fast Algorithm for Particle Simulations. *J. Comput. Phys.*, 73: 325–348, 1987.

[6] R. Illner, P. Dukes, H. D. Victory, and A. V. Bobylev. On Vlasov-Manev equations, II: Local Existence and Uniqueness. *JSP*, to appear, 1998.

[7] G. Manev. La gravitation et le principe de l'égalité de l'action et de la réaction. *Comptes Rendues*, 178: 2159–2161, 1924.

[8] G. Manev. Die Gravitation und das Prinzip von Wirkung und Gegenwirkung. *Zeitschrift für Physik*, 31: 786–802, 1925.

[9] G. Manev. La gravitation et l'eńrgie au zéro. *Comptes Rendues*, 190: 1374–1377, 1930.

[10] G. Manev. Le principe de la moindre action et la gravitation. *Comptes Rendues*, 190: 963–965, 1930.

[11] H. Minc. *Nonnegative Matrices.* J. Wiley & Sons, 1988.

[12] S. Rjasanow. Effective algorithms with circulant-block matrices. *Linear Alg. Appl.*, 202: 55–69, 1994.

[13] C. Van Loan. *Computational Frameworks for the Fast Fourier Transform.* SIAM, Philadelphia, 1992.

R. Illner
Department of Mathematics
and Statistics
University of Victoria
P.O. Box 3045
Victoria, B.C. V8W 3P4
Canada
rillner@Math.UVic.CA

S. Rjasanow
Fachbereich 9 - Mathematik
Universität des Saarlandes
Postfach 151150
66041 Saarbrücken
Germany
rjasanow@num.uni-sb.de